Facial Skin Texture and Distributed Dynamic Kernel Support Vector Machine (DDKSVM) Classifier for Age Estimation in Facial Wrinkles

V. Hemasree[1*] and Dr.K. Sundeep Kumar [2]

[1*]Research Scholar, Computer Science and Engineering, Visvesvaraya Technological University, Jnana Sangama, VTU Main Rd, Machhe, Belagavi, Karnataka, India.
hemasreemuni12@gmail.com

[2]Professor & HOD, Department of Computer Science and Engineering, S.E.A College of Engineering and Technology, K.R. Puram, Banglore, Karnataka, India.
sundeepkumarkk@gmail.com

Received: July 30, 2022; Accepted: September 26, 2022; Published: November 30, 2022

Abstract

Facial wrinkles are common aspects of ageing human skin that may be used in a variety of image-based ageing applications. Wrinkles on the face are 3D skin characteristics that appear as tiny discontinuities or fissures, as well as inconsistencies in the surrounding skin texture. Existing image-based techniques to ageing skin analysis focus on wrinkles as texture rather than curvilinear discontinuity/crack or irregularity characteristics. Picture processing methods are useful for reconstructing and manipulating an image in order to produce various images. The goal of this study is to create a FWDAE-IP (Face Wrinkles Detection and Age Estimate with Image Processing) system that can identify the exact position of wrinkle lines in relation to cracks/ discontinuities, abnormalities, and age estimation using skin texture data from one face image. This FWDAE-IP system is performed based on four major steps: Preprocessing, Skin texture feature extraction, wrinkles detection, and age estimations. In the first step, preprocessing is performed by rotation angle. In the second step, GFs (Gabor Filters), ALTPs (Adaptive Local Ternary Patterns), and AAMs (Active Appearance Models) are introduced against variation in pose or illumination. In the third step, GMM-EM (Gaussian Mixture Model- Expectation-Maximization) is introduced for detecting irregularities in the wrinkles, Gabor filters and image morphology is introduced for detecting discontinuity/crack in the wrinkles. In the fourth step, age estimation is performed based on the detected with wrinkles by DDKSVM (Distributed Dynamic Kernel Support Vector Machine) classifier. The results of age estimation methods are measured via the evaluation metrics such as MAEs (Mean Absolute Error), CSs (Cumulative Scores), accuracy, SSIMs (structural Similarity Indices), and JSIs (Jcard Similarity Indices). The experimentation work is performed based on FG-NET database.

Index Terms: Face Wrinkles Detection and Age Estimation with Image Processing (FWDAE-IP), Adaptive Local Ternary Pattern (ALTP), Distributed Dynamic Kernel Support Vector Machine (DDKSVM), Age Estimation, Skin Texture, and Classifier.

Journal of Internet Services and Information Security (JISIS), volume: 12, number: 4 (November), pp. 84-101
DOI: *10.58346/JISIS.2022.I4.006*

*Corresponding author: Research Scholar, Computer Science and Engineering, Visvesvaraya Technological University, Jnana Sangama, VTU Main Rd, Machhe, Belagavi, Karnataka, India.

1 Introduction

Facial recognitions are biometric recognition technologies with a bright future used in information security, public safety, and other domains. Academicians have been using facial based processing in wide spread areas including facial detections [1], facial recognitions, verifications, tracking [2], recognition of 3D facial expressions [3,4], and other areas related to classical facial analysis. The study of facial like age estimations, gender recognitions, and ethnic recognitions has also generated interest in many researchers [5]. The age of a person is a significant factor in how it connects with others. It divulges details about people's personal lives and socio-cultural origins, as well as human behaviours. Changes in the texture of the skin on the face are generally seen as part of the adult ageing process. However, the degree of ageing is influenced by a variety of factors, including gender, race, heredity, lifestyle, and health state. As a result, age estimate fr5om faces has become a popular study topic in computer vision and can be used in many real-world settings including CRM (customer relationship management), security controls, surveillance, HCIs (human-computer interaction), biometrics, and criminal investigations [6, 7].

Studies on facial age estimations encounter substantial challenges which make most research projects difficult to assess. Existing public facial databases include many problematic elements like age, gender, and ethnicity imbalances. Despite significant challenges, the facial age estimations can be applied in many areas. Facial wrinkles are affected by several factors, but can be strongly linked to ageing, since, certain people appear to have lesser wrinkles than others. The rate of wrinkle growth and its patterns are yet unknown. Wrinkle detections have lately acquired popularity, and numerous automated computerized algorithms to localize wrinkles have been developed [8, 9], though, in a recent study [10], the wrinkle detection algorithms were found to be very reliable. Image preprocessing, feature extraction, and age estimation are all part of the facial age estimate process. Many methods for estimating facial age based on the processes outlined above have been presented during the last decade, but have had limitations:

- The bulk of earlier studies relied solely on frontal datasets for validation.
- The wrinkle identifications were based on wrinkle lines not areas.
- Proposed algorithms couldn't tell the difference between coarse and fine wrinkles.
- Existing algorithms were unable to clearly define wrinkles in terms of cracks, discontinuities, and irregularities.
- However, keep in mind that the approaches utilized in these applications are mostly dependent on using wrinkles as texture characteristics, with just a few attempts to analyse wrinkles as edges/curvilinear objects.
- In general, image-based wrinkle recognition and localization as curvilinear objects has gone unexplored. Though facial wrinkles have textures, it is complex to determine patterns at high resolutions.
- Wrinkles are more properly defined as little discontinuities, flaws, or fissures in the surrounding inhomogeneous skin texture.

This paper proposes FWDAE-IP (Face Wrinkles Detection and Age Estimation with Image processing) system where faces are categorized based on age groups for estimating ages inside the categorized groups. The main four stages of this work are preprocessing, feature extractions, wrinkle detections, and age estimations. Ages are estimated using age groups and estimations. Moreover, the

results are evaluated using metrics such as MAEs, CSs, SSIMs, and JSIs and tested on the FG-NET database.

2 Literature Review

Batool and Chellappa [10] used image morphologies in their proposed scheme for improved localization outcomes. Image features based on GFs outputs gave importance to skin texture's discontinuous curves due to wrinkles with large responses for GFs which were subsequently processed and geometrical constraints curvilinear wrinkle structures were located to image places. The findings of the study's experiments executed on low- and high-resolution Images were compared with MPPs (Marked Point Processes) modeling where resulting experiments revealed that the suggested method not only outperformed MPPs in terms of visual quality and speed.

Jana et al. [11] suggested a technique for estimating a person's true age by examining the wrinkle area of facial photos. From a facial picture, wrinkle geographic regions are recognized, and wrinkle characteristics are retrieved. Each facial picture is grouped using the FCM (Fuzzy C-Means) clustering technique based on wrinkle characteristics where the membership function generated cluster's average age. The study's results obtained are substantial and noteworthy.

Liang et al. [12] established a hierarchical age estimation approach that included age group and particular age estimates. Their proposed approach incorporated two classifications of SKNNs (Sequence K-Nearest Neighbors) and RKNNs (Ranking KNNs) to predict age groups. Instead of treating samples as independent entities, RKNNs leveraged ordinal information between samples in the study's estimations. The study's age group evaluations on the FG-NET database had 4.97 as the value for MAEs (mean absolute errors). The entire age span was split into particular ordinal sub-spans by transforming age labels into category labels during the age group estimation phase which also assisted to mitigate the impact of the present facial dataset's uneven distribution problem. The age evaluation problem was handled by a ranking model that combined a number of ordinal binary classifiers that made use of the ordinal information concealed in ageing processes.

Batool and Chellappa [13] proposed responses and texture orientation from GFs as field image attributes. Bimodal GMMs (Gaussian mixture models) were used to illustrate the Gabor properties of normal skins against its abnormalities. The spatial interactions between neighboring pixels for distributions and texture orientations of GMMs were identified subsequently by MRFs (Markov Random Fields) model. Skin and wrinkles/imperfections were distinguished by the usage of EMs (Expectation-Maximizations). When wrinkles/imperfections are recognized automatically, they are eliminated entirely rather than blended or blurred. To demonstrate the efficacy of suggested methods, results from image analysis are retrieved from the Internet.

Chao et al. [14] suggested a method for estimating age that is distinguished by the following three contributions. The study assessed relationships between facial attributes and age labels baqsed on distances and reduced dimensionalities. Subsequently, in training, label sensitiveness and imbalances were remedied to take advantage of inherent ordinal connections between human's age and data imbalances. The study's final stage was age assessments using local regressions where their experimental results had reduced estimational errors when compared to previous approaches.

According to Hu et al [15], effective preprocessing of ULBPs (Uniform Local Binary Patterns) facial textures can be obtained and they subsequently employed multi-class SVMs (Support Vector Machines) for classifications based on age. The study split subjects are separated into five age groups: children (0–6), juveniles (7–18), youth (18–40), middle-aged (40–65), and old (≥66). For age estimate,

Deng et al [16] suggested a compact multifeature learning and fusion technique. Three sub-networks are presented to learn information about gender, ethnicity, and age. These complementing traits are then combined to generate more robust age estimate features. Lastly, features are converted to accurate age estimated values using regression ranks. In comparison to existing approaches, experimental findings on three benchmark datasets proved the proposed method's efficacy and efficiency in estimating facial ages and consumed only 20 MB of memory making it viable to be used in low memory devices.

For facial age estimations, Liu and Liu [17] used fusions of stages. They began with gender identifications followed by grouping of data specific to genders. These gender groups were then estimated for ages before all three processes were fused in the final stage. The study's experimentations showed improved performances when compared many other age estimation approaches.

Elmahmudi and Ugail [18] used facial templates for their construction of average faces of certain races and ages. Their target aged facial images were generated by applying facial images to appropriate facial image templates. The final image was controlled by textures and shapes. To validate their technique, similarities with old photographs were assessed. The study extracted features using pre-trained CNNs (Convolution Neural Networks) based on the VGG-facial model, which were then compared with other known classifiers. Wang and Chen [19] suggested using extracted textural characteristics and landmarks to predict age using SVMs for regression prediction technique. Their predictions using landmarks in place for textures of faces showed that facial landmarks' morphological qualities reflect facial ages better.

Thus, this review found there was a lack of studies in identifying facial crack/ discontinuities, irregularities, estimation of age from skin texture features. Moreover, studies have been found to be hurdled by two major issues: (1) Analysis of facial wrinkles with respect to crack/ discontinuities, irregularities (2) Estimation of age from skin texture features, since samples are treated as separate people, ordinal information is lost when estimating age from skin texture data. These issues have great impact on age prediction accuracies and have been frequently overlooked.

3 Proposed Methodology

In this work, FWDAE-IP system (Face Wrinkles Detection and Age Estimation with Image processing) is introduced it makes to detection of crack/ discontinuities, irregularities, estimation of age from skin texture features which occur from one facial image. In the proposed system, preprocessing is performed by rotation angle. The texture and contours of a facial picture carry age information. Use Appearance features, such as form features, and GFs and ALTPs for texture feature extraction during the feature extraction phase. For recognizing irregularities in wrinkles, the GMM-EM is used, and for detecting discontinuity/crack in wrinkles, Gabor filters and picture morphology are used. In terms of age estimation, the DDKSVMs classifier is used to estimate age groups and age values. Preprocessing, feature extraction, wrinkle detection, and age estimate are the four primary aspects of the proposed system, as shown in Figure 1.

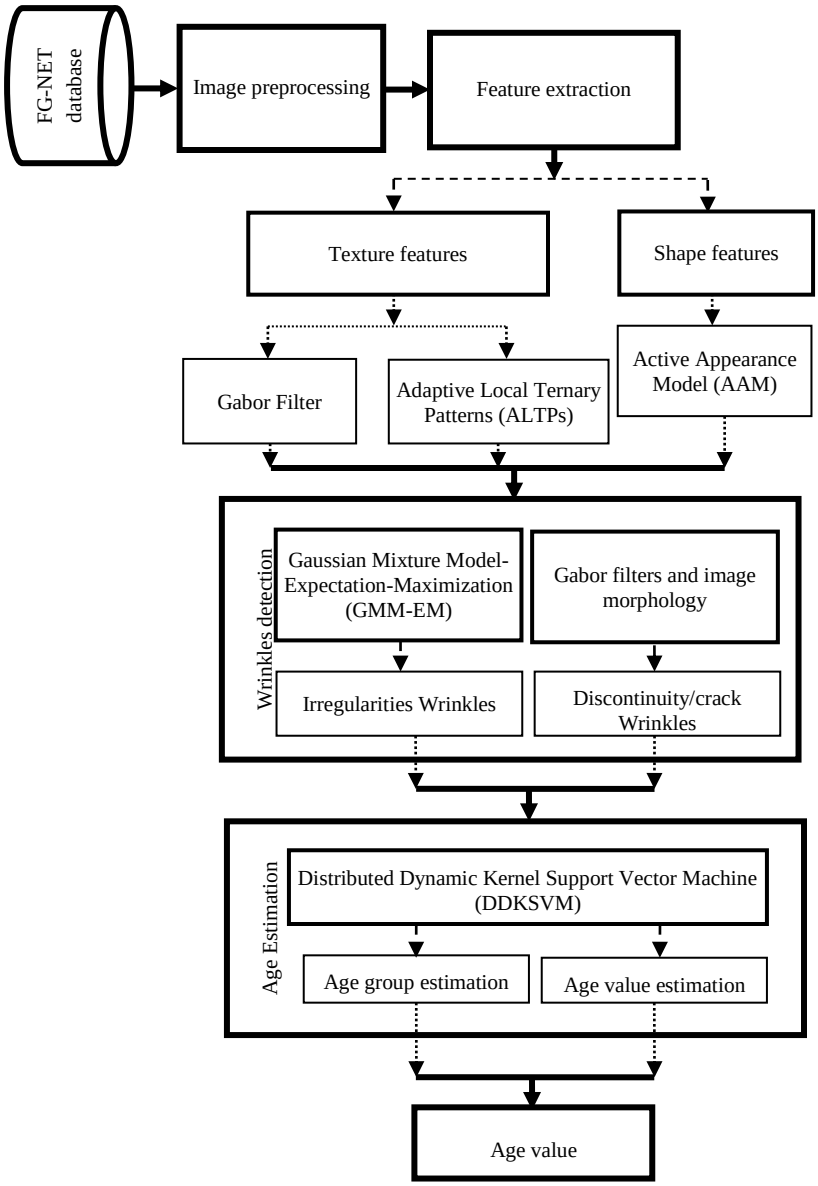

Figure 1: Framework of the Proposed System

3.1. Image Preprocessing

It is complex to force users to maintain frontal facial postures in facial applications and thus precise localization of facial areas and the computation of facial geometric measures becomes very difficult. Conducting sample rotation in-plane can reduce the impacts of non-frontal face positions. Initially, in-plane rotation angle θ can be computed using the positions of two eyes. If the value exceeds a certain threshold value, corrections can be applied to the sample. The threshold was set to 5^0 based on marked deviations of facial landmarks. The computation followed for calculating in-plane rotation angle calculation was:

$$\theta = arg tan \frac{y_L - y_R}{x_L - x_R} \quad (1)$$

Where (x_L, y_L) and (x_R, y_R) are the locations of the left and right eyes, respectively.

3.2. Feature Extraction

Feature extraction is performed by texture and shape features. It is described in the following section.

3.2.1. Texture features

Since, texture descriptors are important to image appearances, this work uses ALTPs and GFs to assess local facial textures for feature extractions.

GFs

GFs are popular feature descriptor based on local features and are robust to pose or illumination variations. Kernel oriented GFs for 2D image planes with an angle α can be depicted as equation (2),

$$G_{ab}(x,y) = \frac{1}{2\pi\sigma_x\sigma_y}\exp\left[-\frac{1}{2}\left(\frac{x'}{\sigma_x^2}+\frac{y'}{\sigma_y^2}\right)\right]\cos(2\pi f x') \tag{2}$$

Where

$$\begin{bmatrix}x'\\y'\end{bmatrix} = \begin{bmatrix}\cos\alpha & \sin\alpha\\ -\sin\alpha & \cos\alpha\end{bmatrix}\begin{bmatrix}x\\y\end{bmatrix} \tag{3}$$

If $\{G_{ab_k}(x,y), k = 0,\cdots,K-1\}$ stands for set of GFs at angles $\alpha_k = -\frac{\pi}{2}+\frac{\pi k}{K}$ where K represents filters in equivalent spaces in the angular interval $\left[\frac{-\pi}{2},\frac{\pi}{2}\right]$. By convolving the GF bank with the provided image, Gabor features can be produced.

LTPs (Local Ternary Patterns) have also been used in this work to study aged skin textures. Because the threshold value is chosen to be the same as the center pixel, Local Binary Patterns (LBPs) are susceptible to noise, especially in near uniform picture areas [21,22]. By using different radius values from the center pixel, LTPs provided better resilience to noises than LBPs. Because many facial areas are homogeneous, LTPs have been proven to give superior effects than LBPs. Equation is used to explain it (4),

$$f_{(P,R)}^{LTP}(p_c) = \sum_{i=0}^{P-1} s(p_i,p_c)2^i \tag{4}$$

$$s_{LTP}(x,p_c) = \begin{bmatrix}1\ if\ x \geq p_c + r\\ 0\ if\ |x-p_c| < r\\ -1\ if\ x \leq p_c - r\end{bmatrix} \tag{5}$$

Ternary patterns can be positive or which are then processed separately as two channels of LBPs and their resulting LBP histograms are for obtaining image features. A localized LTPs threshold selection is used for obtaining ALTPs feature descriptors. While using LTPs, Weber's law was discovered i.e. ratios between increments and background values were constants where Weber's law can be stated as:

$$\frac{\Delta I}{I} = k \tag{6}$$

Where, ΔI represents Weber fraction and noticeable increments difference useful for discriminations; I is the starting background intensity and k implies that left side of the above equation is a constant for different values of I. Weber's law states that noticeable differences in ΔI are constant proportions of original stimulus values and based on Weber's Law, LTPs thresholds can be set using equation (7),

$$t = p_c \times k \tag{7}$$

Where k is the Weber's law parameter. Since the threshold in LTPs could be automatically set, the method is called Adaptive Local Ternary Patterns (ALTP).

The χ^2 histogram distance is described by equation (8),

$$\chi^2(p,q) = \sum_i \frac{(p_i - q_i)^2}{p_i + q_i} \tag{8}$$

ALTPs for facial recognition:

Step 1. Compute LTPs thresholds using equation (7);

Step 2. Compute image ALTPs and obtain coded images;

Step 3. Split the obtained coded image into m*n cells;

Step 4. Compute histograms of cells and concatenate them to obtain total histogram or final features;

Step 5. Classify using nearest neighbor classifiers using histogram distances χ^2

3.2.2. Shape features

AAMs are introduced in this work to detail statistical generative model of facial shapes and textures/ intensities [23,24] as they are popular facial descriptors and use PCAs (Principle Component Analysis) for reducing dimensionalities which maintain important facial structures in images. Building AAMs based models require annotated image sets where images have their landmark facial points marked. AAMs models process shapes and appearances discretely where shapes are learnt prior marked landmark point coordinates. Assuming N_T and N_L denote trainingimage count and count of landmark points in training facial imagea and $\boldsymbol{p} = [x_1, y_1, x_2, y_2, \ldots, x_{N_L}, y_{N_L}]^T$ is a vector of length $2N_L \times 1$ representing landmark's planar coordinates. Shapes get created first using Generalized Procrustes Analysis which aligns N_T training forms while PCAs alignshapes for obtaining N_T eigenvectors, $\in \mathcal{R}^{2N_L \times N_T}$ with mean shape being p. Appearances are regenerated by warping training images onto mean forms where pixels lying inside mean shape p is denoted by N_A and if $\boldsymbol{l}(\boldsymbol{x}), \boldsymbol{x} \in \boldsymbol{p}$ stands for vector of length $N_A \times 1$ representing the intensity/appearance values of the N_A pixels within the form's models for the appearance, then models are trained similiarly to obtain appearance for N_T eigenvectors, $E_a \in \mathcal{R}^{N_A \times N_T}$ and $\bar{l}$ the mean appearance . Thus, on learning shapes and appearancesby AAMs, new instances $(p*, l*)$ can be synthesized or represented as linear combinations of eigenvectors weighed by the model parameters depicted as equation (9),

$$p* = \bar{p} + E_s a \tag{9}$$

$$l* = \bar{l} + E_l b \tag{10}$$

Where **a** and **b** are the shape and appearance parameters respectively.

3.3. Wrinkles Detection

Each sample has a matching file in the FG-NET ageing database, which records sixty-eight facial feature points. From these sixty-eight sites, eight distances may be determined using fifteen landmarks. However, sample size might affect the distance between particular spots, causing shape description to be unstable. Applying form ratios instead of lengths between facial feature points is an excellent way to get rid of the picture scale dependency and where 8 distances are computed for obtaining 6 ratios. Since, curvilinear objects, have algorithms that can locate discontinuities caused in wrinkled faces,

their localizations enable a variety of applications linked to ageing skin, facial biometrics, and skin recognition and monitoring as people age.

3.3.1. Image Features and GFs

GFs highlight facial wrinkles curvilinear features in this work and GF's kernel oriented at angle α is given by equation (11),

$$g(x_1, x_2) = \frac{1}{2\pi\sigma_{x_1}\sigma_{x_2}} exp\left[-\frac{1}{2}\left(\frac{x_1'^2}{\sigma_{x_1}^2} + \frac{\gamma^2 x_1'^2}{\sigma_{x_2}^2}\right)\right] cos(2\pi f x_1') \tag{11}$$

Where the parameters σ_{x_1}, σ_{x_2} denote the scale of the 2D Gaussian envelope, f denotes the frequency of the sinusoid and γ denotes the spatial aspect ratio which defines the ellipticity or the elongation of support of Gabor function. The values for x_1, x_2 are given by equation (12),

$$\begin{bmatrix} x_1' \\ x_2' \end{bmatrix} = \begin{bmatrix} \cos\alpha & \sin\alpha \\ -\sin\alpha & \cos\alpha \end{bmatrix} \begin{bmatrix} x_1 \\ x_2 \end{bmatrix} \tag{12}$$

Assuming$\{g_k(x_1, x_2), k = 0, \dots, K-1\}$ represent GFs oriented at angles $\alpha_k = -\frac{\pi}{2} + \frac{\pi k}{K}$ and K *stands for* equally spaced filter counts in angular interval $\left[\frac{-\pi}{2}, \frac{\pi}{2}\right]$ and $\{I(x_1, x_2);\ x_1 = 1 \dots N_1, x_2 = 1 \dots N_2\}$ denotes gray scale image inputs then filtered image using $g_k(x_1, x_2)$ is $I_k^F(x_1, x_2)$ and where relevant maximum amplitude of filtered responses can be depicted by equation (13),

$$I'(x_1, x_2) = \max_k I_k^F(x_1, x_2) \tag{13}$$

The maximum amplitude response is normalized to the range [0, 1] according to the following equation (14-15),

$$I^{"}(x_1, x_2) = (I'(x_1, x_2) - \min_{(x_1, x_2)} I'(x_1, x_2))^p \tag{14}$$

$$I^N(x_1, x_2) = \frac{I^{"}(x_1, x_2)}{\max_{(x_1, x_2)} I^{"}(x_1, x_2)} \tag{15}$$

Where p >1 for highlighting image spots with greater GFs responses. Initially, regions of forms are searched around end point's linked components based on orientations of connected components. The two components are united if an adjacent connected component has an end point. By diluting each linked component with a rectangular section, a non-overlapping area is obtained. Any segments of wrinkle curves that overlap these locations are eliminated during extension and drifting.

3.3.2. Image morphology

Image morphology emphasizes geometrical constraints to localize wrinkle's curvilinear shapes in large GF response regions of images.

3.3.3. Gaussian Mixture Model- Expectation-Maximization (GMM-EM)

GMM-MRF (Gaussian Mixture Model based on Markov Random Field) has been proposed in this work for obtaining spatial smoothness constraints in neighboring pixels [25]. MRF model's prior distributions of pixel mixes (x_1, x_2), denoted by π_{x_1,x_2}^j, is based on their neighbors and hence prior joint distribution of π_{x_1,x_2}^j for all pixels given by Gibbs distribution stated below:

$$p(\prod|\mathfrak{T}', \Theta) \propto p(\mathfrak{T}'|\prod, \Theta) \times p(\prod) \tag{16}$$

$$p(\mathfrak{T}'|\prod,\Theta)=\prod_{x_!=1}^{N_1}\prod_{x_2=1}^{N_2}\sum_{j=1}^{J}\pi_{x_1,x_2}^{j}\Phi(I'(x_1,x_2)|\mu^j,\sigma^j) \tag{17}$$

$$p(\prod)=\frac{1}{Z}\exp\left(-\frac{U(\prod)}{T}\right) \tag{18}$$

Where Z is the normalization constant, U(Π) is the Gibbs energy function and T is a constant called temperature. According to equation (16), (17) and (18), the posteriori log-density function can be derived as,

$$L(\prod|\mathfrak{T}',\Theta)=\log p(\prod|\mathfrak{T}',\Theta)=\prod_{x_!=1}^{N_1}\prod_{x_2=1}^{N_2}\sum_{j=1}^{J}\pi_{x_1,x_2}^{j}\Phi(I'(x_1,x_2)|\mu^j,\sigma^j)-logZ-\frac{U(\prod)}{T} \tag{19}$$

EMs are generally used for distribution estimations of GMMs. However, incorporating prior distributions of GMMs through MRFs adds complexity and M steps of EMs cannot estimate model parameters directly from data. Hence, different approximations have been suggested to handle this issue where Nguyen et al. [25] proposed a unique method for adding spatial correlations to MRFs that allowed for a near form solution during Maximizations. Their addition variable G_{x_1,x_2}^{j} to the equation is as follows,

$$G_{x_1,x_2}^{j}=exp\left\{\frac{\beta}{2|\mathcal{N}_{x_1,x_2}}\sum_{i\in\{\mathcal{N}_{x_1,x_2}\}}(z_i^j+\pi_i^j)\right\} \tag{20}$$

Where $\mathcal{N}_{x_1,x_2}$ is the neighborhood of the pixel (x_1, x_2) and z_i^j is the posterior probability. The factor G_{x_1,x_2}^{j} is the averaging process promotes smoothing of prior probability since it is proportional to the product of both posterior probabilities and prior distributions of surrounding pixels. Nguyen et al. presented a novel Gibbs energy function update at an EM iteration t based on the EM method G_{x_1,x_2}^{j} as follows [25],

$$U^{(t+1)}(\prod|\mathfrak{T}',\Theta)\ =-\prod_{x_!=1}^{N_1}\prod_{x_2=1}^{N_2}\sum_{j=1}^{J}G_{x_1,x_2}^{j,(t)}\log\pi_{x_1,x_2}^{j,(t+1)} \tag{21}$$

The factor $G_{x_1,x_2}^{j,(t)}$ is solely determined by priors and posteriors calculated in the preceding stage of the EM method. This provides for a more straightforward and closed-form technique for updating mixing proportions π_{x_1,x_2}^{j}.

Fusion of Gabor Features and Texture Orientation Field: Though in GMM-MRF models, pixels share globally distributed Gaussian parameters i.e. Θ, pixels have different mix proportions, π_{x_1,x_2}^{j}, instead of the global values. Modifications by Nguyen et al [25] to GMM-MRF model for fusing texture orientations with Gabor features resulted in better detections when compared to unmodified GMM-MRF models. The texture orientation field, $\theta(x_1,x_2)$, is considered a priori field affecting the prior probabilities of mixing proportions. Let $\Omega=\{\theta_{x_1,x_2}\,;\,x_1=1,\cdots,N_1;\,x_2=1,\cdots,N_2\}$ denote the set of orientation angles of all pixels.

$$p(\prod,\Theta|\mathfrak{T}',\Omega)\propto p(\mathfrak{T}'|\prod,\Theta,\Omega)\times p(\prod|\Omega) \tag{22}$$

$$U(\prod,\Omega)=-\sum_{x_1}^{N_1}\sum_{x_2}^{N_2}\sum_{j=1}^{J}G_{x_1,x_2}^{j}(\Omega)\log\pi_{x_1,x_2}^{j} \tag{23}$$

$$p(\prod|\Omega) = \frac{1}{Z}\exp\left(-\frac{U(\prod|\Omega)}{T}\right) \tag{24}$$

Introduce the factor $G^{j}_{x_1,x_2}$ as a function of theorientation field Ω and is given as follows,

$$G^{j}_{x_1,x_2} = exp\left\{\sum_{i\in\{\mathcal{N}_{x_1,x_2}\}} h(j,\theta_i)(z_i^j + \pi_i^j)\right\} \tag{25}$$

The factor $h(j,\theta_i)$ The orientation field angles in a pixel's vicinity are used to regulate the mixing proportions of that pixel. The factor is specified in the binary case, where j = 0 signifies the distribution representing background skin and j = 1 denotes the distribution representing wrinkled skin as follows,

$$h(j,\theta_i) = \begin{cases} 1\ for\ j = 0 \\ \beta\ cos\theta_i for\ j = 1 \end{cases} \tag{26}$$

From this discontinues of the wrinkles are detected.

3.4. Age Estimation

DDKSVMs have been proposed in a simple extension of basic SVMs. Suppose that the input age space $x \in \mathbb{R}^n$ and a set of age image samples $x_1, \dots, x_r$ are given. The identifier function is given by equation (27),

$$f(x) = w^T x - b \tag{27}$$

The coefficient w is a weight and b is a non-negative bias. $d-1$ dimensional hypersurface identifier that satisfies f(x)=0 is described by equation (28),

$$\{x \in: (w^T x) + b = 0\} \tag{28}$$

When training input images $(x_1, y_1), \dots, (x_l, y_l), x_i \in \{i = 1, \dots N\}, y_i \in \{\pm 1\}, i = 1, \dots l$ are given and consider the problem to identify the identifier function.

$$f_{w,b} = sgn((w.x) + b)) \tag{29}$$

That satisfies,

$$f_{w,b}(x_i) = y_i, i = 1, \dots . l \tag{30}$$

For this identifier function, set the constraints of following equation (31),

$$y_i(w^T x_i + b) \leq 1, i = 1, \dots . l \tag{31}$$

In this case, the distance between the identifier surface (margin) and these hyper surfaces is $\frac{1}{\|w\|}$. So, the problem to find the parameters that maximize margin, results in finding the parameters that minimize the objective function,

$$\tau(w) = \frac{1}{2}\|w\|^2 \tag{32}$$

Under the constraint of equation (31). Introduce the Lagrange multipliers $\alpha_i (\geq 0)$ and rewrite the objective function by equation (33),

$$L(w,b,\alpha) = \frac{1}{2}\|w\|^2 - \sum_{i=1}^{l} \alpha_i\{y_i((w^T x_i) + b) - 1\} \tag{32}$$

From partial differentiation with respect to $w$and b, obtain by equations (33),

$$w = \sum_{i=1}^{l} \alpha_i y_i x_i \tag{33}$$

Substituting these to the objective function gives the dual problem,

$$L_D(\alpha) = \sum_{i=1}^{l} \alpha_i - \frac{1}{2} \sum_{i,j=1}^{l} \alpha_i \alpha_j y_i y_j x_i^T x_j \tag{34}$$

Under the constraints,

$$\sum_{i=1}^{l} \alpha_i y_i = 0 \tag{35}$$

$$0 \le \alpha_i, i = 1, \dots l \tag{36}$$

w is obtained from optimal $\alpha$by using equation (33) and $b$is given by equation (37),

$$b = \frac{1}{2}(w^T x_{+1} + w^T x_{-1}) \tag{37}$$

Here, x_{+1}, $x_{-1}$are support vectors belonging to the class 1, -1. Suppose x_{+1}denotes an image dataset with age labels larger than class and x_{-1} denotes animage dataset with age labels no more than class. Using kernel, the objective function is represented by equation (38),

$$L_D(\alpha) = \sum_{i=1}^{N} \alpha_i - \frac{1}{2} \sum_{i,j=1}^{N} \alpha_i \alpha_j t_i t_j \phi(x_i^T) \phi(x_j) = \sum_{i=1}^{N} \alpha_i - \frac{1}{2} \sum_{i,j=1}^{N} \alpha_i \alpha_j t_i t_j K(x_i, x_j) \tag{38}$$

And the optimal identifier function is obtained by equation (39),

$$f(x) = sign\left(\sum_{i=1}^{l} \alpha_i y_i \phi(x_i)^T \phi(x) + b \right) = sign\left(\sum_{i=1}^{l} \alpha_i y_i K(x_i, x) + b \right) \tag{39}$$

In dynamic SVM criterion, they assume that data and parameters are dynamic, and they consider that these transit with conditional probabilities. They assume a priori parametric distribution of the instances,

$$\phi(x|a_t, b_t, y; c) = const., yz(a_t, x) \le 1, \exp\left(-c\left(1 - yz(a_t, x)\right)\right), yz(a_t, x) < 1 \tag{40}$$

The objective function is computed by equation (41),

$$\begin{aligned} J\left(a_t, b_t, \delta_{t,j}, t = 0, \dots, T\right) & \\ = a_0^T a_0 + \frac{1}{d} \sum_{t=1}^{T} (a_t - q a_{t-1})^T (a_t - q a_{t-1}) + \frac{1}{d'} \sum_{t=1}^{T} (b_t - b_{t-1})^2 & \\ + \sum_{t=1}^{T} \sum_{j=1}^{N_t} \delta_{j,t} & \end{aligned} \tag{41}$$

$$\rightarrow \min_{[a_t, b_t]_{t=1}^T} y_{j,t}\left(a_t^T x_{j,t} + b_t\right) \le 1 - \delta_{j,t}, \delta_{j,t} \le 0, j = 1, \dots . N_t, t = 1, \dots T \tag{42}$$

$$z(x, a_t) = a_t^T x + b = 0 \tag{43}$$

Dynamic SVM is the assumption of distributing kernel [26]. The problem is represented as follows [27],

$$\max W(\alpha) = \sum_{i=1}^{n_x} \alpha_i - \frac{1}{2} \sum_{i,j=1}^{n_x} \alpha_i \alpha_j y_i y_j \exp\left\{ -\frac{\left| x_i - x_j \right|^2}{\sigma_i \sigma_j} \right\}, 0 \le \alpha_i \le C, \sum_{i=1}^{n_x} \alpha_i y_i = 0 \tag{44}$$

The identifier function is described by equation (45),

$$f(x) = sgn\left[\sum_{i=1}^{n_x} exp\left\{-\frac{|x_i - x_j|^2}{\sigma_i \sigma_j}\right\} + b^*\right] \tag{45}$$

Although this is the same form with basic SVM, but the difference is the assumption of data which follows dynamic process. The data transit from x_i to x_j with the changes of time from i to j, following the distribution by equation (46),

$$exp = exp\left\{-\frac{|x_i - x_j|^2}{\sigma_i \sigma_j}\right\} \tag{46}$$

This can be used for age estimation. First, in the age group estimation step, set all age values into an ordinal category sequence and then map category labels into different age groups by DDKSVM.

4 Experiments and Analysis

In this part, compare the proposed system to current approaches using the widely used FG-NET ageing dataset from https://yanweifu.github.io/FG NET data/. The FG-NET ageing dataset has 1002 photos of 82 people (6-18 images per person) ranging in age from 0 to 69 years (FG-NET ageing dataset, accessed on September 2012). On all of the facial photos, the collection additionally includes 68 landmark characteristics that were manually detected. In addition, all of the photographs in the collection have the following meta-data: image size, age, gender, spectacles, hat, moustache, beard, horizontal pose, and vertical position. The facial photographs include all potential variants, including lighting, position, emotion, beards, moustaches, spectacles, and so on, because they were gathered from real-life albums of various topics.

4.1. Performance evaluation metrics

The results of methods are measured via using evaluations of SSIMs, JSIs, MAEs, CSs, and accuracies.

SSIMs: are used to calculate similarities between ground truths and new faces.

JSIs: are tools for determining the reliability of wrinkle detection methods. The intersection of A and B divided by the union of A and B yields the Jaccard index J. Annotations A and B are from two separate programmers, respectively. Equation is used to define it (47),

$$J(\mathrm{A}, B) = \frac{|A \cap B|}{|A \cup B|} \tag{47}$$

Accuracy: In order to validate the correctness of the proposed method, accuracy is defined by equation (48),

$$Acc = \sum_{i=1}^{N} w_i \, , w_i = \begin{cases} 1 \; if \; JSI_i > 40\% \\ 0 \; else \end{cases} \tag{48}$$

Where N is the total number of photos in the experiment and w denotes if the JSI is greater than 40%. Correct detection is defined as any overlap between A and B that is more than or equal to 40%.

MAEs: The average of the absolute errors between the estimated agelabels and ground truth age labels results in MAEs. Equation is used to explain it (49),

$$MAE = \sum_{i=1}^{N} \left(\frac{|A_i - B_i|}{N}\right) \tag{49}$$

Where $B_k$is the ground truth age for the k-th test image, A_k is the estimated age, and Nis the total number of test images.

CSs: can be defined by equation (50),

$$CS(j) = \frac{N_{e \leq j}}{N} * 100 \quad (50)$$

Where $N_{e \leq j}$ is the number of test photos where the age estimator produces an absolute error of no more than j years. The classification accuracy can also disclose the age estimation performance as a classification challenge. If an ordinal label is provided in a large training data set with a dense range of ages, CS may be the best technique to represent performance.

Input image-01	AAM	Gabor features	Forehead	Segmented image
	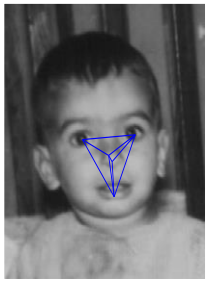	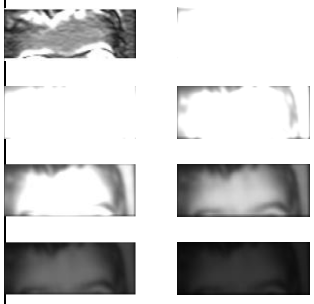		 Age: 02 No wrinkles
Input image-01	**AAM**	**Gabor features**	**Forehead**	**Segmented image**
		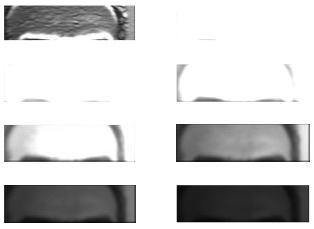		 Age: 43 Wrinkles
Input image-17	**AAM**	**Gabor features**	**Forehead**	**Segmented image**
		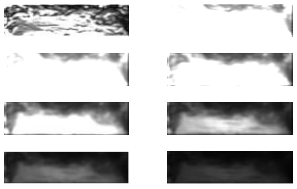		 Age: 42 Wrinkles
Input image-06	**AAM**	**Gabor features**	**Forehead**	**Segmented image**
	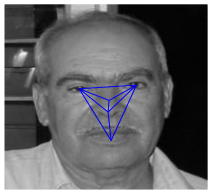	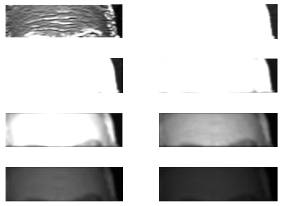		 Age: 69 Wrinkles

Figure 2: Image Results with Stages

Figure 2 shows the results of input images with steps like AAMs for shape feature extractions, Gabor features, head foreheads, and wrinkles detections with respect to the rows 2,3,4,5.

Table 1: Performance Evaluation Metrics

METHODS	SSIM	JSI	ACCURACY	CS	MAE	TIME (SECONDS)
MPP	0.8096	0.5323	0.7729	0.8881	2.6610	40.5645
SKNN	0.8291	0.6184	0.8169	0.9017	1.8712	35.9297
RKNN	0.8904	0.6294	0.8441	0.9322	1.2475	32.7062
SVM	0.9080	0.6534	0.8780	0.9390	1.0847	30.7463
DDKSVM	0.9454	0.6881	0.9119	0.9661	0.6780	21.8834

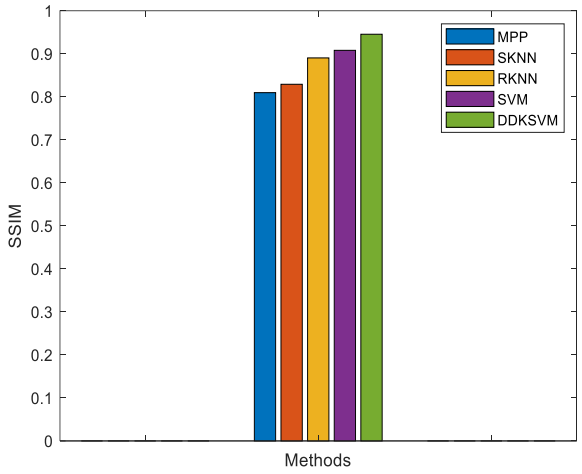

Figure 3: Structural Similarity Index (SSIM) Comparison of Age Estimation Methods

Figure 3 shows the performance comparison results of age estimation methods with respect to SSIM metric. The methods like MPP, SKNN, RKNM, SVM and proposed DDKSVM is evaluated under FG-NET database. The proposed DDKSVM classifier gives higher SSIM value of 94.54%, whereas other methods such as MPP, SKNN, RKNM, SVM has lesser SSIM value of 80.96%, 82.91%, 89.04%, and 90.80% respectively (See Table 1).

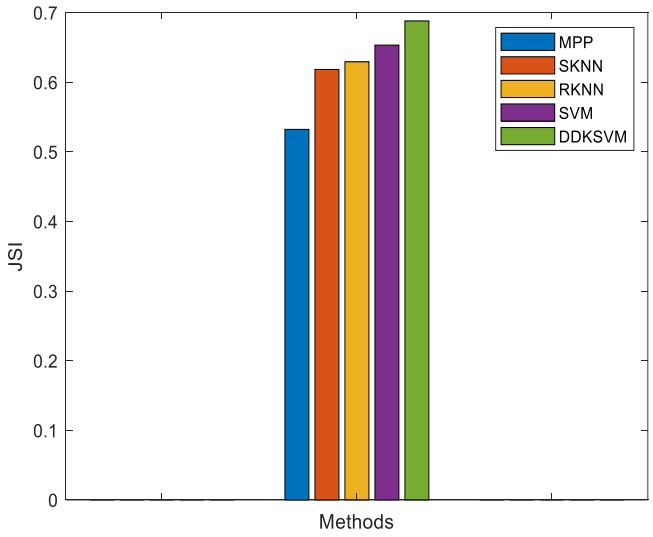

Figure 4: Jaccard Similarity Index (JSI) Comparison of Age Estimation Methods

JSI results comparison with respect to age estimation methods are illustrated in figure 4. The methods like MPP, SKNN, RKNM, SVM, and proposed DDKSVM is evaluated under FG-NET database. The proposed DDKSVM classifier gives higher JSI value of 68.81%, whereas other methods such as MPP, SKNN, RKNM, SVM has lesser SSIM value of 53.23%, 61.84%, 62.94%, and 65.34% respectively (See Table 1).

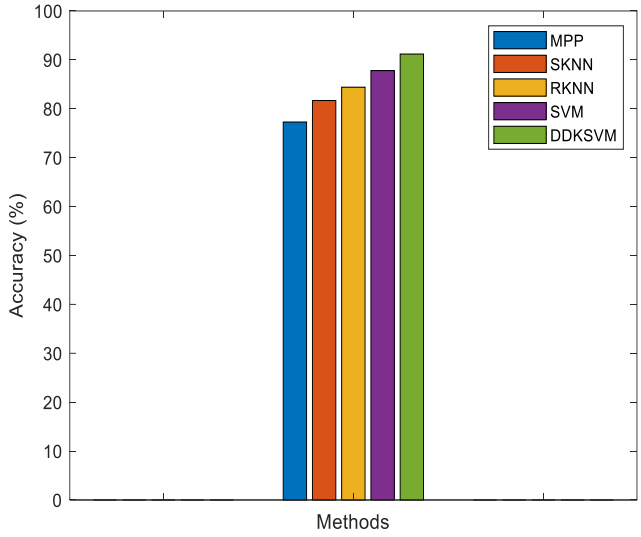

Figure 5: Accuracy Comparison of Age Estimation Methods

Overall accuracy with respect to age estimation methods are illustrated in figure 5. The estimation methods like MPP, SKNN, RKNM, SVM, and proposed DDKSVM is evaluated under FG-NET database. The proposed DDKSVM classifier provides higher accuracy of 91.19%, whereas other methods such as MPP, SKNN, RKNM, SVM has lesser accuracy value of 77.29%, 81.69%, 84.41%, and 87.80% respectively (See Table 1). The proposed algorithm has higher results than the other methods due to crack, irregularities detection of wrinkles via GMM-EM, and Gabor filters.

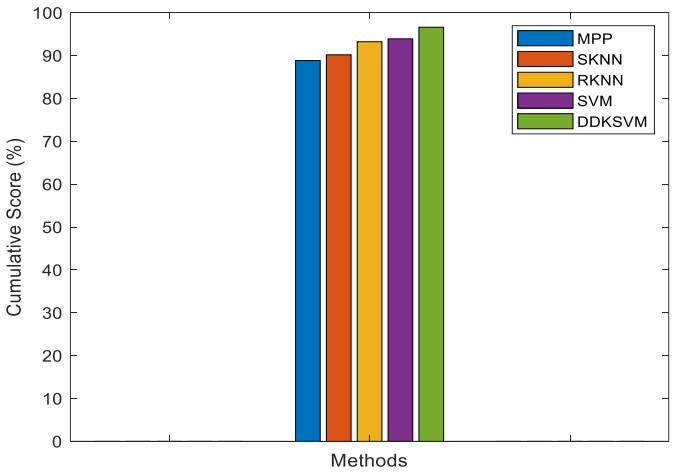

Figure 6: Cumulative Score Comparison of Age Estimation Methods

Age estimation methods with respect to cumulative score are illustrated in figure 6. The age estimation methods like MPP, SKNN, RKNM, SVM and proposed DDKSVM is evaluated under FG-NET database. The proposed DDKSVM classifier provides CS of 96.61%, whereas other methods such as MPP, SKNN, RKNM, SVM has lesser CS value of 88.81%,90.17%,93.22%, and 93.90%

respectively (See Table 1). The proposed algorithm has higher results than the other methods due to crack, irregularities detection of wrinkles.

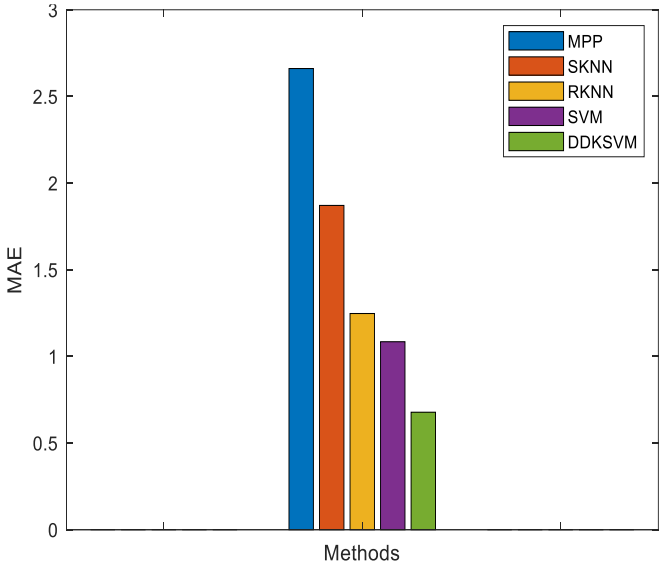

Figure 7: Mean Absolute Error (MAE) Comparison of Age Estimation Methods

The Mean Absolute Error (MAE) results comparison of age estimation methods such as MPP, SKNN, RKNM, SVM and proposed DDKSVM with respect to FG-NET database is shown in figure 7. The proposed DDKSVM classifier provides lesser MAE value of 0.6780, whereas other methods such as MPP, SKNN, RKNM, SVM has higher MAE value of 2.6610,1.8712, 1.2475, and 1.0847 respectively (See Table 1).

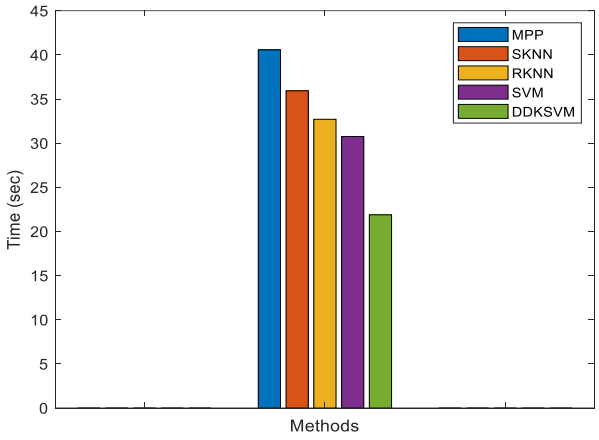

Figure 8: Time Comparison of Age Estimation Methods

Figure 8 shows the performance comparison of time metric with respect to age estimation methods. Age estimation methods, time comparison is varied from one method to another method due to training and testing. The proposed DDKSVM has taken lesser time of 21.8834 seconds, other methods such as MPP, SKNN, RKNM, and SVM consumes higher time of 40.5645 seconds, 35.9297 seconds, 32.7062 seconds, and 30.7463 seconds respectively (See Table 1). Since the proposed work, different form of prediction is performed which may increases the results and reduces the time of the system.

5 Conclusion and Future Work

This research offers a Distributed Dynamic Kernel Support Vector Machine-based age estimation methodology (DDKSVM). Preprocessing is done via rotation angle in the suggested system. Shape and texture features are retrieved from the preprocessed picture during the feature extraction step. Gabor Filter, ALTPs is used to extract textural features from a facial picture. Active Appearance Model (AAM) to the research of facial age estimate for shape feature extraction. In wrinkle detection, Gaussian Mixture Model- Expectation-Maximization (GMM-EM) is introduced for detecting irregularities in the wrinkles. Moreover, Gabor filters and image morphology is introduced for detecting discontinuity/crack in the wrinkles. Based on detected wrinkles, Distributed Dynamic Kernel Support Vector Machine (DDKSVM) was used for age estimation. In DDKSVM criterion. They consider that data and parameters are dynamic and that they transit with conditional probability. Experiments reveal that during the training phase, the suggested system converges rapidly, has high accuracy, higher similarity, and a lower Mean Absolute Error (MAE) during the age estimation phase. We will focus more on sample preparation in the future, given the significant impact of facial occlusion, emotion, and position. At the same time, we'll work to improve the group estimation method, as the outcome has a significant impact on the whole system's performance.

References

[1] Klare, B.F., Klein, B., Taborsky, E., Blanton, A., Cheney, J., Allen, K., & Jain, A.K. (2015). Pushing the frontiers of unconstrained face detection and recognition: Iarpa janus benchmark a. *In Proceedings of the IEEE conference on computer vision and pattern recognition*, 1931-1939.

[2] Cao, C., Hou, Q., & Zhou, K. (2014). Displaced dynamic expression regression for real-time facial tracking and animation. *ACM Transactions on graphics (TOG)*, *33*(4), 1-10.

[3] Vezzetti, E., Tornincasa, S., Moos, S., Marcolin, F., Violante, M.G., Speranza, D., & Padula, F. (2016). 3D human face analysis: Automatic expression recognition. *Biomedical engineering*, 2016-832.

[4] Vezzetti, E., & Marcolin, F. (2014). 3D Landmarking in multi expression face analysis: a preliminary study on eyebrows and mouth. *Aesthetic plastic surgery*, *38*(4), 796-811.

[5] Guo, G., & Mu, G. (2014). A framework for joint estimation of age, gender and ethnicity on a large database. *Image and Vision Computing*, *32*(10), 761-770.

[6] Angulu, R., Tapamo, J.R., & Adewumi, A.O. (2018). Age estimation via face images: a survey. *EURASIP Journal on Image and Video Processing*, *2018*(1), 1-35.

[7] Liu, K.H., Yan, S., & Kuo, C.C.J. (2015). Age estimation via grouping and decision fusion. *IEEE Transactions on Information Forensics and Security*, *10*(11), 2408-2423.

[8] Cula, G.O., Bargo, P.R., Nkengne, A., & Kollias, N. (2013). Assessing facial wrinkles: automatic detection and quantification. *Skin Research and Technology*, *19*(1), 243-251.

[9] Ng, C.C., Yap, M.H., Costen, N., & Li, B. (2015). Wrinkle detection using hessian line tracking. *IEEE Access*, *3*, 1079-1088.

[10] Batool, N., & Chellappa, R. (2015). Fast detection of facial wrinkles based on Gabor features using image morphology and geometric constraints. *Pattern Recognition*, *48*(3), 642-658.

[11] Jana, R., Datta, D., & Saha, R. (2015). Age estimation from face image using wrinkle features. *Procedia Computer Science*, *46*, 1754-1761.

[12] Liang, Y., Wang, X., Zhang, L., & Wang, Z. (2014). A hierarchical framework for facial age estimation. *Mathematical problems in Engineering*, *2014*(242846), 1-8.

[13] Batool, N., & Chellappa, R. (2014). Detection and inpainting of facial wrinkles using texture orientation fields and Markov random field modeling. *IEEE transactions on image processing*, *23*(9), 3773-3788.

[14] Chao, W.L., Liu, J.Z., & Ding, J.J. (2013). Facial age estimation based on label-sensitive learning and age-oriented regression. *Pattern Recognition*, *46*(3), 628-641.
[15] Hu, L., Li, Z., & Liu, H. (2015). Age group estimation on single face image using blocking ULBP and SVM. *In Proceedings of the Chinese Intelligent Automation Conference*, 431-438. Springer, Berlin, Heidelberg.
[16] Deng, Y., Teng, S., Fei, L., Zhang, W., & Rida, I. (2021). A multifeature learning and Fusion Network for Facial Age estimation. *Sensors*, *21*(13), 4597.
[17] Liu, K.H., & Liu, T.J. (2019). A structure-based human facial age estimation framework under a constrained condition. *IEEE Transactions on Image Processing*, *28*(10), 5187-5200.
[18] Elmahmudi, A., & Ugail, H. (2021). A framework for facial age progression and regression using exemplar face templates. *The visual computer*, *37*(7), 2023-2038.
[19] Wang, M., & Chen, W. (2021). Age prediction based on a small number of facial landmarks and texture features. *Technology and Health Care*, *29*(S1), 497-507.
[20] Lu, J., Liong, V.E., & Zhou, J. (2015). Cost-sensitive local binary feature learning for facial age estimation. *IEEE Transactions on Image Processing*, *24*(12), 5356-5368.
[21] Preethi, P., Asokan, R., Thillaiarasu, N., & Saravanan, T. (2021). An effective digit recognition model using enhanced convolutional neural network based chaotic grey wolf optimization. *Journal of Intelligent & Fuzzy Systems*, (Preprint), 1-11.
[22] Preethi, P., & Asokan, R. (2021). Modelling LSUTE: PKE Schemes for Safeguarding Electronic Healthcare Records Over Cloud Communication Environment. *Wireless Personal Communications*, *117*(4), 2695-2711.
[23] Smolyanskiy, N., Huitema, C., Liang, L., & Anderson, S.E. (2014). Real-time 3D face tracking based on active appearance model constrained by depth data. *Image and Vision Computing*, *32*(11), 860-869.
[24] Zhou, H., Lam, K.M., & He, X. (2016). Shape-appearance-correlated active appearance model. *Pattern Recognition*, *56*, 88-99.
[25] Nguyen, T.M., & Wu, Q.J. (2012). Fast and robust spatially constrained Gaussian mixture model for image segmentation. *IEEE transactions on circuits and systems for video technology*, *23*(4), 621-635.
[26] Guangzhi, S., Lianglong, D., Junchuan, H., & Yanxia, Z. (2010). Dynamic support vector machine by distributing kernel function. *In IEEE 2nd International Conference on Advanced Computer Control*, *2*, 362-365.
[27] Sato, M. (2016). Derivation of kernel of dynamic support vector machines: Stochastic and deterministic data process. *Peer J Pre Prints*, *4*, 1-13.
[28] Manfredi, S., Ceccato, M., Sciarretta, G., & Ranise, S. (2022). Empirical Validation on the Usability of Security Reports for Patching TLS Misconfigurations: User-and Case-Studies on Actionable Mitigations. *Journal of Wireless Mobile Networks, Ubiquitous Computing, and Dependable Applications*, *13*(1), 56-86.